UC Davis
UC Davis Previously Published Works

Title

Toll-like receptor 4 and myeloid differentiation factor 88 are required for gastric bypass-induced metabolic effects

Permalink

https://escholarship.org/uc/item/55v3n8tv

Journal

Surgery for Obesity and Related Diseases, 17(12)

ISSN

1550-7289

Authors

Abu El Haija, Marwa
Ye, Yuanchao
Chu, Yi
et al.

Publication Date

2021-12-01

DOI

10.1016/j.soard.2021.07.019

Peer reviewed

VA Author Manuscript

Toll-like receptor 4 and myeloid differentiation factor 88 are required for gastric bypass-induced metabolic effects

Marwa Abu El Haija, M.D.[#a,b], **Yuanchao Ye, Ph.D.**[#c], **Yi Chu, Ph.D.**[c], **Hussein Herz, M.S.**[c], **Benjamin Linden, B.S.**[c], **Shailesh K. Shahi, Ph.D.**[d], **Kasra Zarei, M.S.**[e], **Ashutosh K. Mangalam, Ph.D.**[d,f], **Steven J. Mcelroy, M.D.**[a,g], **Mohamad Mokadem, M.D.**[c,h,i,j,*]

[a]Stead Family Department of Pediatrics, University of Iowa Carver College of Medicine, Iowa City, Iowa

[b]Department of Pediatrics, Division of Gastroenterology, Hepatology, and Nutrition, Stanford University School of Medicine & Lucile Packard Children's Hospital, Palo Alto, California

[c]Department of Internal Medicine, University of Iowa Carver College of Medicine, Iowa City, Iowa

[d]Department of Pathology, University of Iowa Carver College of Medicine, Iowa City, Iowa

[e]Medical Scientist Training Program, University of Iowa Carver College of Medicine, Iowa City, Iowa

[f]Interdisciplinary Graduate Program in Immunology and Molecular Medicine, University of Iowa Carver College of Medicine, Iowa City, Iowa

[g]Department of Microbiology and Immunology, University of Iowa Carver College of Medicine, Iowa City, Iowa

[h]Fraternal Orders of Eagles Diabetes Research Center, University of Iowa, Iowa City, Iowa

[i]Obesity Research & Education Initiative, University of Iowa, Iowa City, Iowa

[j]Veterans Affairs Health Care System, Iowa City, Iowa

[#] These authors contributed equally to this work.

Abstract

Background: Toll-like receptor 4 (TLR4) has been suggested as one of the forefront cross-communicators between the intestinal bacteria and the host to regulate inflammatory signals and energy homeostasis. High-fat diet–induced inflammation is mediated by changes in gut microbiota and requires a functional TLR-4, the deficiency of which renders mice resistant to diet-induced obesity and its associated metabolic dysfunction. Furthermore, gut microbiota was suggested to

*Correspondence: Mohamad Mokadem, M.D., University of Iowa, 200 Hawkins Drive, 4570 JCP, Iowa City, Iowa 52242. mohamad-mokadem@uiowa.edu (M. Mokadem).

play a key role in the beneficial effects of Roux-en-Y gastric bypass (RYGB), a commonly performed bariatric procedure.

Objectives: To explore whether TLR4, myeloid differentiation factor 8 (MyD88; 1 of its key downstream signaling regulators) and gut microbiota play an integrative role in RYGB-induced metabolic outcomes.

Setting: Animal-based study.

Method: We performed RYGB in TLR4 and MyD88 knock-out (KO) mice and used fecal microbiota transplant (FMT) from RYGB-operated animals to these genetic mouse models to address our questions.

Results: We demonstrate that RYGB reduces TLR4 expression explicitly in the small and large intestine of C57Blc/6J mice. We also show that TLR4 KO mice have an attenuated glucoregulatory response to RYGB. In addition, we reveal that MyD88 KO mice fail to respond to all RYGB-induced metabolic effects. Finally, fecal microbiota transplant from RYGB-operated mice into TLR4 KO and MyD88 KO naïve recipients fails to induce a metabolic phenotype similar to that of the donors, as it does in wild-type recipients.

Conclusion: TLR4 and MyD88 are required for RYGB-induced metabolic response that is likely mediated by gut microbiome.

Keywords

Obesity has been closely associated with a state of low-grade inflammation that is orchestrated by the innate immune system, which seems to play a role in development of insulin resistance. Toll-like receptor 4 (TLR-4) has been recognized as 1 of the key players in this regulation. TLR-4 was also shown to be an important link between diet-induced changes in gut microbiome and resulting systemic inflammation [1,2]. Several markers of chronic inflammation were found to be elevated in serum and adipose tissue of children and adults with obesity [3–10]. Innate immune responses can be initiated by activation of TLR4 via lipopolysaccharide that are produced by gram-negative bacteria [2]. TLR4 is mainly expressed in innate immune cells such as monocytes, macrophages, and dendritic cells as well as adipocytes [11] and, in addition to lipopolysaccharide, can be activated by saturated fatty acids [2,12,13]. Once activated, TLR4 launches a cascade of immune responses that end up activating nuclear factor kappa B either through a myeloid differentiation factor 88 (MyD88)-dependent or -independent pathway [2]. Several studies in the literature already suggest that TLR4 and its downstream regulators (such as MyD88) play a role in energy and glucose homeostasis For example, animals lacking a functional TLR4 are relatively protected from a high-fat diet (HFD)-induced obesity and diabetes [14–18]. Interestingly, animals lacking TLR5, which is mainly MyD88 dependent, are at increased risk for obesity [19].

Gut-residing microbiota was shown to play an important regulatory role in development and progression of obesity and its associated metabolic disorders [20–22]. Moreover, alteration in gut microbiota, which is induced by a HFD, requires a functional TLR4 to influence

weight balance, glucose metabolism, and the resultant systemic inflammation that has been previously associated with diet-induced obesity [2,4].

Bariatric surgery was shown to be 1 of the most effective available therapies for weight loss as well as for treatment of type 2 diabetes [23,24]. Roux-en-Y gastric bypass (RYGB) is 1 of the 2 most common bariatric surgeries performed, and it has more durable effects on weight and resolution of diabetes than sleeve gastrectomy, the other commonly performed bariatric procedure [25–27]. Gut microbiota has been implicated not only in obesity development but also in the mechanism involving its reversal such as after RYGB [28]. It is unclear, however, if gut microbiome-mediated improvements in energy and glucose homeostasis post-RYGB involve a crosstalk with the innate immune system through TLR4 signaling. We examine whether the metabolic regulatory effects of RYGB require TLR4 signaling by using TLR4 knock-out (KO) and MyD88 KO mice. Finally, to examine the role of microbiota in this interaction, we study the effect of fecal/microbial transfer of RYGB-operated animals into naïve wild-type (WT) recipients in comparison to those lacking TLR4 or MyD88.

Methods

Animals

All animal care and procedures have been approved by the affiliated Institution Animal Care and Use Committee/IACUC. Five-to 6-week-old male WT C57Bl/6J TLR4 KO (TLR$^{4tm1.2Karp}$; stock no. 029015), and MyD88 KO (MyD88$^{tm1.1Defr/J}$; stock no. 009088) on the same background were purchased from Jackson Laboratory. Animals were placed on a HFD (Research Diets, Inc. D12492, 60% Kcal from fat) at age 6 weeks and continued on same diet until completion of the study. The mice were maintained on 12-hour light–dark cycle and were provided with water 24 hours a day. Diet-induced obese (DIO) mice were randomly selected to undergo RYGB or sham surgery. Mice were placed liquid diet (Ensure from Abbott) during the first week of surgical recovery, and then a solid HFD was resumed on day 8 and maintained until conclusion of all studies. Food intake was measured on postoperative week 3 between 9:00 and 9:30 AM for 5 days by subtracting the amount of high fat remained from the amount weighed in, corrected for the spillage found in the cage floor. Stool were collected at the same time and stored at −80°C for later use for the fecal microbiota transplant (FMT) experiment (see following discussion).

Roux-en-Y-gastric bypass surgery in mice

RYGB surgical procedure is performed according as described in previous work [29,30]. Specifically, animals received a presurgical 12-hour fast, and all mice were given enrofloxacin for antibiotic prophylaxis and buprenorphine for analgesia. Anesthesia was provided using isoflurane inhalation system (5% for induction and 1%–2% for maintenance). Eye ointment was applied as part of the preparation of the animal. The abdomen was sterilized and prepped by (1) removing hair with an electric razor, (2) 3 steps of scrubbing with betadine, and (3) wiping with alcohol. Laparotomy was performed using forceps and scissors and extended from the xiphoid to umbilicus. After identification of the ligament of Treitz, intestine was transected 5 cm distal to the ligament using surgical microscissors, and then a jejunojejunostomy was performed by end-to-side anastomosis

with an 8–0 monofilament (Monosof or ETHILON). Subsequently, the stomach was freed from its ligamentous attachments to the liver and spleen. Gastrojejunostomy was performed after introduction of enterotomy using surgical scissors. The second anastomosis was performed also with an 8–0 monofilament using a running suture. Gastric exclusion was then performed using a vascular hemostasis clip applied from the greater curve to the lesser curve along the posterior border of the fundus. The abdominal vagus was preserved. Clip was sutured in place using 5–0 VICRYL. Closure was performed using 40 VICRYL (or polydioxanone) with a running suture (for abdominal wall) and interrupted sutures using 4–0 nylon plus Vetbond tissue adhesive from 3M (for the skin). Before closure of abdominal wall, the peritoneal cavity was filled with sterile normal saline (.9%NaCl) to provide hydration for the early postoperative period.

Study design

Eighteen-to 19-week-old DIO WT mice, weighing 39 to 45 g, were randomized to undergo RYGB or sham surgery. Similar weight-matched MyD88 KO and TLR4 KO mice were also randomized to RYGB or sham surgery. Because TLR4 KO are resistant to obesity, they took longer time to reach the goal weight; hence, their ages were 22 to 24 weeks.

During postoperative week 1, a once-daily injection of analgesics was given for 2 days and then on an as-needed basis. All mice were placed on liquid diet and intra-peritoneal dextrose injections for this first week. During postoperative week 2, they recovered in their home cages on a solid HFD until sacrifice. During postoperative weeks 3 to 6, all experiments (as described in the following text) were performed. At the end of 6 weeks, animals were sacrificed, and tissue and blood were harvested.

Metabolic profile testing

Glucose tolerance tests (GTT)/insulin tolerance tests (ITT) were performed. GTT was performed following an overnight fast for 16 hours (postsurgery weeks 4 and 5), mice received 1g/kg D-glucose (cat no: 50–99-7, RPI, Mt. Prospect, IL) by oral gavage. Blood glucose was measured from tail vein blood using a handheld glucometer (Contour) immediately before and 15, 30, 60, 90, and 120 minutes after glucose administration.

ITT was performed following a 4-hour fast (postoperative weeks 5 and 6). Mice received .75 U/kg insulin (NDC 0002–8215-01, HI-210, Humulin R, Eli Lily) by intraperitoneal injection. Blood glucose was measured from tail vein blood using a handheld glucometer (Contour) immediately before and 15, 30, 60, 90, and 120 minutes after glucose administration.

Energy expenditure measurement

Measurements of energy expenditure (EE), respiratory exchange rate, VO_2 and VCO_2 were obtained using the CLAMs system, which relies on indirect calorimetry (respirometry) for energy assessment, within the Metabolic Phenotyping Core Facility. All mice were individually housed for 5 days in standard housing premeasurement for acclimatization; they were then moved into free-running metabolic cages with 24-hour access to food and water where all study data were continuously recorded 24 hours per day for another 5 days.

Immunohistochemistry

Paraffin-embedded tissues were stained for TLR4 by blocking with peroxide and then permeabilizing the tissue with .4% triton-X and phosphate-buffered saline/Tween. After that, the sample was incubated overnight at 4°C with the primary antibody [TLR4/Novus (76B357.1) at 1:400 dilution]. Thereafter, horseradish peroxidase secondary antibody (antimouse for TLR4) was added for 30 minutes at room temperature followed by 3,3′-diaminobenzidine before the tissue analysis.

Western blot

For western blot and protein extraction, tissues were homogenized in tissue lysis buffer (50 mM 4-[2-hydroxyethyl]-1-piperazineethanesulfonic acid, pH7.5, 150 mM NaCl, 1 mM $MgCl_2$, 1 mM $CaCl_2$, 10 mM NaF, 5 mM ethylenediaminetetraacetic acid, 1% Triton X-100, 2 mM sodium orthovanadate, and Roche cocktail protease inhibitor tablet). Protein samples (50 μg) were injected to 8% sodium dodecyl-sulfate polyacrylamide gel electrophoresis gel, electro transferred to a polyvinylidene fluoride membrane (Bio-Rad). After blocking with 5% w/v nonfat dry milk in tris-buffered saline/Tween (.1% Tween 20), membrane was probed with anti-TLR4 (Lot: CJZU03–06, Cat: NB100–56566, Novus Biologicals) or β-actin (Proteintech, Cat 60008–1-Ig, 1:500,000) overnight at 4°C, followed with antimouse antibody (1:10,000) at room temperature for 2 hours. Visualization was performed with enhanced chemiluminescence detection kit (GE healthcare) followed by autoradiography.

Fecal microbiota transplant experiment

Wild-type, TLR4 KO, and MyD88 KO mice on regular chow diet received fecal transplant from sham- or RYGB-operated mice when they were 8 weeks old according to previously published protocol [31]. Fecal material (.3 g) from RYGB- and sham-operated mice was collected. Pooled, sterile mortar and pestle were used for grounding, and fecal material was suspended in sterile water (1 mL/.1 g stool). Samples were centrifuged for 2 minutes at $3000 \times g$ to remove large particulates. Individual mice received 100 μL of respective fecal supernatant by oral gavage daily for 14 consecutive days. Weight, food intake, and feeding efficiency were calculated.

Gut hormone measurement

Serum was collected from mice that underwent overnight fasting and stored at −80°C and concentrations of glucagon-like peptide 1, gastric inhibitory polypeptide, leptin, and ghrelin were measured using a magnetic bead multiplex assay (Bio-plex Pro mouse diabetes assay, Cat no. 171F7001M, Bio-Rad). Procedures were followed according to Bio-Rad instruction manual, and final measurement was performed on a Luminex 200 instrument at the Flow Cytometry Core of the University of Iowa. Serum concentrations of peptide YY (PYY) were measured using a mouse PYY enzyme immunoassay kit (EIAM-PYY, RayBiotech) following the manufacturer's instruction. Briefly, serum, as well as standards and positive control, were mixed with a constant concentration of biotinylated peptide (PYY). The mixes were incubated in wells coated with an anti-PYY antibody, to which PYY in serum and biotinylated PYY were competitively bound. Biotinylated PYY was then quantified with

streptavidin horseradish peroxidase, followed by a color reaction in standard enzyme-linked immunosorbent assay.

Microbiota sequencing analysis

After mice were sacrificed, their ceca were collected on the spot and immediately snap-frozen in liquid nitrogen to be later stored at −80°C. Microbiome analysis was done as described previously [32]. Briefly, extraction of microbial DNA from cecal samples was performed using DNeasy PowerLyzer PowerSoil Kit (Qiagen) followed by amplification and sequencing of the 16s ribosomal RNA V3–V4 region on an Illumina MiSeq platform at Iowa Institute of Human Genetics. Raw 16s sequence data were processed by R script Divisive Amplicon Denoising Algorithm 2 to generate amplicon sequence variants, which were then assigned taxonomies using a naive Bayesian classifier with the Silva database as a reference [33]. Analysis of these data was then conducted using online microbiome tools METAGENassist [34] and MicrobiomeAnalyst [35].

Statistical analysis

All data points are expressed as mean ± standard error of the mean (SEM) and analyzed by Student's *t* tests or 1- or 2-way analysis of variance (ANOVA), which was followed by Tukey–Kramer post hoc analysis when appropriate. Statistical analyses were performed using GraphPad Prism 9.0 (GraphPad software). A $P<.05$ was considered statistically significant. Analysis of covariance was used to correct EE data for body mass using SPSS, as indicated in Figs. 1 to 6. This approach is recommended by field magnates in the recent article "Guide to Analysis of Mouse Energy Metabolism" manuscript published in *Nature Methods* [36].

Results

TLR4 expression is decreased in the luminal gut post-RYGB

We first examined the effect of RYGB on TLR4 expression in multiple tissues and found that TLR4 is decreased in the small intestine and large intestine (colon) of DIO mice postsurgery as evidenced by Western blot (Fig. 1) and immunohistochemistry (Supplementary Fig. 1). No significant change in TLR4 expression was observed in the liver, pancreas, subcutaneous, mesenteric, or gonadal white adipose tissue (WAT) (Fig. 1).

TLR4 is required for RYGB-induced metabolic effects

Effect on weight balance and food intake—To examine the role of TLR4 in regulating the metabolic effects of RYGB, we used TLR4 KO mice on C57/Blc/6J background. We placed them on a HFD to induce obesity, and as previously reported, they proved to be resistant to weight gain (Fig. 2A). They also had lower fasting insulin and lower homeostatic model assessment for insulin resistance (Fig. 2B). Given the fact that TLR4 KO and WT mice gain weight at different rates on a HFD, we selected a weight-matched group from both sides to perform the RYGB study. We found that TLR4 KO mice lost less percentage weight compared with their WT counterparts post-RYGB (Fig. 2C and 2D). The average daily food intake was decreased in TLR4 KO mice compared to the WT group, while no effect on energy consumption was observed due to RYGB surgery

itself (Fig. 2E). The decrease in feeding efficiency, however, which was also previously reported in WT obese mice post-RYGB [29,30] was no longer detected in TLR4 KO mice (Fig. 2F).

Energy expenditure and glucose homeostasis

Effect on energy expenditure and glucose homeostasis—To further characterize the effect of TLR4 in metabolic regulation of energy balance post-RYGB, we placed both WT and TLR4 KO groups in metabolic cages. We found that the increase in EE and the change in O_2 and VCO_2 exchange rates observed post-RYGB in WT mice are lacking in the TLR4 KO group (Fig. 3A–3C). The baseline EE and respiratory exchange ratio were lower in TLR4 KO mice and were not affected by RYGB surgery (Fig. 3A–3C). As for glucose metabolism, the oral GTT improved in both WT and TLR4 KO mice post-RYGB (Fig. 3D). However, interestingly, the intraperitoneal ITT improved only in WT and not TLR4 KO mice postsurgery (Fig. 3E). It is important to note that while all mice were weight-matched preprocedure, the TLR4 KO mice were older.

MyD88 KO mice lack complete response to RYGB surgery—Because TLR4 can signal and activate nuclear factor kappa B through a MyD88-dependent or -independent pathway, we decided to examine the metabolic effects of RYGB in MyD88 KO DIO mice. We found that MyD88 KO mice have a significantly attenuated weight response to RYGB compared to their WT counterparts. At week 5 postsurgery the difference in preoperative weight between RYGB- and sham-operated mice was only 6.9% in MyD88 KO mice compared to 34.4% in the WT group (Fig. 4A). Similar to the TLR4 KO group, the average daily food intake was reduced compared to WT group, but it was unchanged by the RYGB intervention (Fig. 4B). Feeding efficiency, EE, respiratory exchange ratio, VO_2, and VCO_2 were also unchanged in the MyD88 mice post-RYGB when compared to their WT counterparts (Fig. 4C–4F). Similarly, no improvement in either oral GTT or intraperitoneal ITT was observed in MyD88 KO mice after RYGB (Fig. 4G and 4H).

Gut microbiota-induced metabolic effects require TLR4 and MyD88—Finally, to explore whether RYGB-induced changes in gut microbiota mediate their energy balance effects through TLR4 and its downstream MyD88-dependent pathway, we performed an FMT experiment from RYGB- and sham-operated animals, grouped as WT, TLR4 KO, and MyD88 KO recipients. A diversity score plot shows that RYGB-FMT recipients and sham-FMT recipients resemble their donors more than the donor of their counterpart in term of bacterial diversity and composition (Fig. 5). Also, relative analysis of phyla abundance-using 16s RNA gene sequencing reconfirms previous published data reporting a decrease in Firmicutes/Bacteroidetes ratio post-RYGB and a separate increase in the abundance of the *Proteobacteria* phylum (Supplementary Fig. 2) [30,37–40]. WT mice recipients of RYGB-FMT maintained a stable weight over 2 weeks of fecal gavage while the sham-FMT recipients gained (.9 g ± .3 g). Interestingly, their food intake was similar while the RYGB-FMT recipients expressed a significantly reduced feeding efficiency (Fig. 6A). Remarkably, when the same FMT was performed in TLR4 KO and MyD88 KO mice, no effect was observed on weight balance or feeding efficiency (Fig. 6B and 6C). In fact, surprisingly,

MyD88 KO recipients of RYGB-FMT gained more weight than their sham-FMT recipient counterparts (Fig. 6C).

Discussion

TLR4 has gained an increased amount of attention in the past decade as an important player in energy metabolism by regulating inflammatory pathways within macrophages and other key cells that can affect peripheral and central insulin activity [41]. It has also been linked to gut microbiol—induced inflammation that is specifically related to a HFD [4]. Our study explores the role of TLR4 in the underlying mechanism of RYGB-induced metabolic effects, which were previously associated with changes in gut microbiome [28,40]. Here we show that RYGB induces a reduction in intestinal TLR4 expression but not in the liver or any other subtype of WAT. Similarly, a recent study in human subjects showed that RYGB reduces the level of multiple TLRs (including most specifically TLR4) within the duodenum, jejunum, and ileum of diabetic women with obesity [42].

We also show that TLR4 KO mice have an attenuated response to the weight loss effects and, most remarkably, the glucose regulatory effects of gastric bypass. We specifically demonstrate that TLR4 KO mice lose the RYGB-specific increase in EE. Despite the attenuated effect, TLR4 KO mice did lose some weight, which is most likely due to the transient reduction in food intake induced by RYGB over the first 14 postoperative days, as we previously demonstrated [29,30]. Interestingly, despite the weight loss, TLR4 KO mice displayed a significantly attenuated response to ITT, suggesting a minimal or lack of improvement in insulin sensitivity post-RYGB (Fig. 3E). This result suggests that TLR4 may have a weight-independent role in glucose homeostasis (specifically insulin sensitivity) post-RYGB. Curiously, prior research shows that diabetes remission in women with obesity who underwent RYGB is linearly correlated with a more pronounced reduction in TLR4 expression within the small intestine [42], again associating the glucose regulation post–gastric bypass to TLR4 signaling. Remarkably, RYGB tends to reduce TLR4 expression in the gut, which seems to correlate with diabetes remission, at least in humans. However, complete loss of TLR4 signaling seems to be detrimental to glucose homeostasis after surgery, suggesting that RYGB requires a minimum level of TLR4 function to induce its glucoregulatory effects.

We also demonstrate that RYGB loses its complete metabolic effects in MyD88 KO mice where weight loss is significantly mitigated, and most remarkably, there is no improvement in glucose homeostatic measures post-RYGB in MyD88-deficient animals. This observation also suggests that there could be other TLRs involved in RYGB-mediated regulation of energy and glucose metabolism. Thus, we can conclude that TLR4 and MyD88 are required for RYGB-induced metabolic effects. This finding is also supported by previous findings showing that defective T-cell signaling within the gut (specifically lacking MyD88) predisposes to age-related obesity and diabetes. This mechanism has also been shown to be dependent on luminal gut microbiota [43,44]. Moreover, both TLR4 KO and MyD88 KO mice showed significant reduction in food intake when compared to the WT group, a finding that is not further altered by RYGB surgery. This reduction in energy consumption is not likely related to any changes in gut hormones that might have been induced by genetic

manipulation of these strains because serum PYY, glucagon-like peptide 1, and ghrelin levels were similar among all groups (Supplementary Fig. 3A–3C). In addition, serum leptin levels were, in fact, lower in MyD88 KO and TLR4 KO (Supplementary Fig. 3D). These lower leptin levels likely represent a secondary adaptive mechanism due to the already reduced food intake, the mechanism of which is yet to be identified.

As previously mentioned, the diet-induced obesity changes in gut microbiota have been shown to be dependent on TLR4 signaling [2,4,16]. In addition, gut microbiome has been also suggested to play a regulatory role in gastric bypass–induced metabolic changes [28]. Next, we demonstrate through an FMT study that gut microbiome derived from RYGB-operated animals can convey the energy balance phenotype of the donor to the recipient mice. This microbiota-induced change in energy balance requires both TLR4 and MyD88. Although we did not perform our microbiome transplant experiment in germfree mice, this fecal transfer model of donors mice into conventionalized animals over a 2-week period has been used successfully before with reported replication of the biome transferred and the observed physiologic phenotype in vivo [31]. Interestingly, the MyD88 KO recipients of RYGB-FMT seem to gain more weight than their sham counterparts. This finding is also consistent with the very minimal weight loss response observed in MyD88 KO mice post-RYGB. These 2 observations reinforce (1) the role of MyD88 and hence, indirectly, other TLRs in energy regulation post–gastric bypass and (2) the important contribution of gut microbiota in this interaction between the luminal environment post-RYGB and the host via a MyD88-dependent signaling.

Conclusion

We conclude that although TLR4 expression is reduced within the small intestine post-RYGB, its signaling seems to be required to regulate the metabolic outcomes of gastric bypass surgery. The fact that MyD88 KO mice had more pronounced mitigation to RYGB-induced effects suggests that other TLRs (primarily MyD88 dependent) are likely involved in RYGB mechanism of energy and glucose regulation. One postulated theory of RYGB-induced metabolic regulation could be due to changes in gut microbiome, which communicates new energy signals with the host's TLR signaling pathway in a MyD88-dependent manner. Further studies examining the downstream regulators of this pathway would be paramount to uncover the mechanistic details of this durable effective metabolic procedure.

Supplementary Material

Refer to Web version on PubMed Central for supplementary material.

Acknowledgments

References

[1]. Shi H, Kokoeva MV, Inouye K, Tzameli I, Yin H, Flier JS. TLR4 links innate immunity and fatty acid-induced insulin resistance. J Clin Invest 2006;116(11):3015–25. [PubMed: 17053832]

[2]. Velloso LA, Folli F, Saad MJ. TLR4 at the crossroads of nutrients, gut microbiota, and metabolic inflammation. Endocr Rev 2015;36(3):245–71. [PubMed: 25811237]

[3]. Carolan E, Hogan AE, Corrigan M, et al. The impact of childhood obesity on inflammation, innate immune cell frequency, and metabolic microRNA expression. J Clin Endocrinol Metab 2014;99(3):E474–8. [PubMed: 24423308]

[4]. Kim K-A, Gu W, Lee I-A, Joh E-H, Kim D-H. High fat diet-induced gut microbiota exacerbates inflammation and obesity in mice via the TLR4 signaling pathway. PLoS One 2012;7(10):e47713.

[5]. Varma MC, Kusminski CM, Azharian S, et al. Metabolic endotoxaemia in childhood obesity. BMC Obes 2015;3:3. [PubMed: 26819711]

[6]. Ouchi N, Parker JL, Lugus JL, Walsh K. Adipokines in inflammation and metabolic disease. Nat Rev Immunol 2011;11(2):85–97. [PubMed: 21252989]

[7]. Wolowczuk I, Verwaerde C, Viltart O, et al. Feeding our immune system: impact on metabolism. Clin Dev Immunol 2008;2008:639803.

[8]. Izaola O, de Luis D, Sajoux I, Domingo JC, Vidal M. [Inflammation and obesity (lipoinflammation)]. Nutr Hosp 2015;31(6):2352–8. [PubMed: 26040339]

[9]. Monteiro R, Azevedo I. Chronic inflammation in obesity and the metabolic syndrome. Mediators Inflamm 2010;2010:289645.

[10]. Kuroda M, Sakaue H. Adipocyte death and chronic inflammation in obesity. J Med Invest 2017;64(3–4):193–6. [PubMed: 28954980]

[11]. Lu YC, Yeh WC, Ohashi PS. LPS/TLR4 signal transduction pathway. Cytokine 2008;42(2):145–51. [PubMed: 18304834]

[12]. Huang S, Rutkowsky JM, Snodgrass RG, et al. Saturated fatty acids activate TLR-mediated proinflammatory signaling pathways. J Lipid Res 2012;53(9):2002–13. [PubMed: 22766885]

[13]. Pal D, Dasgupta S, Kundu R, et al. Fetuin-A acts as an endogenous ligand of TLR4 to promote lipid-induced insulin resistance. Nat Med 2012;18(8):1279–85. [PubMed: 22842477]

[14]. Davis JE, Gabler NK, Walker-Daniels J, Spurlock ME. Tlr-4 deficiency selectively protects against obesity induced by diets high in saturated fat. Obesity (Silver Spring) 2008;16(6):1248–55. [PubMed: 18421279]

[15]. Camandola S, Mattson MP. Toll-like receptor 4 mediates fat, sugar, and umami taste preference and food intake and body weight regulation. Obesity (Silver Spring) 2017;25(7):1237–45. [PubMed: 28500692]

[16]. Pierre N, Deldicque L, Barbé C, Naslain D, Cani PD, Francaux M. Toll-like receptor 4 knockout mice are protected against endoplasmic reticulum stress induced by a high-fat diet. PLoS One 2013;8(5):e65061.

[17]. Jia L, Vianna CR, Fukuda M, et al. Hepatocyte Toll-like receptor 4 regulates obesity-induced inflammation and insulin resistance. Nat Commun 2014;5:3878. [PubMed: 24815961]

[18]. Li J, Chen L, Zhang Y, et al. TLR4 is required for the obesity-induced pancreatic beta cell dysfunction. Acta Biochim Biophys Sin (Shanghai) 2013;45(12):1030–8. [PubMed: 23985305]

[19]. Vijay-Kumar M, Aitken JD, Carvalho FA, et al. Metabolic syndrome and altered gut microbiota in mice lacking Toll-like receptor 5. Science 2010;328(5975):228–31. [PubMed: 20203013]

[20]. Cani PD, Bibiloni R, Knauf C, et al. Changes in gut microbiota control metabolic endotoxemia-induced inflammation in high-fat diet-induced obesity and diabetes in mice. Diabetes 2008;57(6):1470–81. [PubMed: 18305141]

[21]. Cavalcante-Silva LHA, Galvão JGFM, Santos de França da Silva JSDF, de Sales-Neto JM, Rodrigues-Mascarenhas. Obesity-driven gut microbiota inflammatory pathways to metabolic syndrome. Front Physiol 2015;6:341. [PubMed: 26635627]

[22]. Flier JS, Mekalanos JJ. Gut check: testing a role for the intestinal microbiome in human obesity. Sci Transl Med 2009;1(6):6ps7.

[23]. Schauer PR, Bhatt DL, Kirwan JP, et al. Bariatric surgery versus intensive medical therapy for diabetes—5-year outcomes. N Engl J Med 2017;376(7):641–51. [PubMed: 28199805]

[24]. Ruiz-Cot P, Bacardí-Gascón M, Jiménez-Cruz A. Long-term outcomes of metabolic and bariatric surgery in adolescents with severe obesity with a follow-up of at least 5 years: a systematic review. Surg Obes Relat Dis 2019;15(1):133–44. [PubMed: 30514669]

[25]. Mohit B, Reddy M, Kosta S, Mathur W, Fobi M. Laparoscopic sleeve gastrectomy versus laparoscopic gastric bypass: a retrospective cohort study. Int J Surg 2019;67:47–53. [PubMed: 31121327]

[26]. Maciejewski ML, Arterburn DE, Van Scoyoc L, et al. Bariatric surgery and long-term durability of weight loss. JAMA Surg 2016;151(11):1046–55. [PubMed: 27579793]

[27]. Gu L, Huang X, Li S, et al. A meta-analysis of the medium- and long-term effects of laparoscopic sleeve gastrectomy and laparoscopic Roux-en-Y gastric bypass. BMC Surg 2020;20(1):30. [PubMed: 32050953]

[28]. Liou AP, Paziuk M, Luevano Jr J-M, Machineni S, Turnbaugh PT, Kaplan LM. Conserved shifts in the gut microbiota due to gastric bypass reduce host weight and adiposity. Sci Transl Med 2013;5(178):178ra41.

[29]. Mokadem M, Zechner JF, Margolskee RF, Drucker DJ, Aguirre V. Effects of Roux-en-Y gastric bypass on energy and glucose homeostasis are preserved in two mouse models of functional glucagon-like peptide-1 deficiency. Mol Metab 2014;3(2):191–201. [PubMed: 24634822]

[30]. Ye Y, Abu El Haija M, Morgan DA, et al. Endocannabinoid receptor-1 and sympathetic nervous system mediate the beneficial metabolic effects of gastric bypass. Cell Rep 2020;33(4):108270.

[31]. Bahr SM, Weidemann BJ, Castro AN, et al. Risperidone-induced weight gain is mediated through shifts in the gut microbiome and suppression of energy expenditure. EBioMedicine 2015;2(11):1725–34. [PubMed: 26870798]

[32]. Shahi SK, Zarei K, Guseva NV, et al. Microbiota Analysis Using Two-step PCR and Next-generation 16S rRNA Gene Sequencing. J Vis Exp 2019;(152). 10.3791/59980.

[33]. Callahan BJ, McMurdie PJ, Rosen MJ, et al. DADA2: high-resolution sample inference from Illumina amplicon data. Nat Methods 2016;13(7):581–3. [PubMed: 27214047]

[34]. Arndt D, Xia J, Liu Y, et al. METAGENassist: a comprehensive web server for comparative metagenomics. Nucleic Acids Res 2012;40(Web Server issue):W88–95. [PubMed: 22645318]

[35]. Dhariwal A, Chong J, Habib S, et al. MicrobiomeAnalyst: a web-based tool for comprehensive statistical, visual and meta-analysis of microbiome data. Nucleic Acids Res 2017;45(W1):W180–8. [PubMed: 28449106]

[36]. Tschöp MH, Speakman JR, Arch JR, et al. A guide to analysis of mouse energy metabolism. Nat Methods 2011;9(1):57–63. [PubMed: 22205519]

[37]. Guo Y, Huang ZP, Liu CQ, et al. Modulation of the gut microbiome: a systematic review of the effect of bariatric surgery. Eur J Endocrinol 2018;178(1):43–56. [PubMed: 28916564]

[38]. Shao Y, Ding R, Xu B, et al. Alterations of gut microbiota after Roux-en-Y gastric bypass and sleeve gastrectomy in Sprague-Dawley rats. Obes Surg 2017;27(2):295–302. [PubMed: 27440168]

[39]. Davies NK, O'Sullivan JM, Plank LD, et al. Altered gut microbiome after bariatric surgery and its association with metabolic benefits: a systematic review. Surg Obes Relat Dis 2019;15(4):656–65. [PubMed: 30824335]

[40]. Wagner NRF, Zaparolli MR, Cruz MRR, et al. Postoperative changes in intestinal microbiota and use of probiotics in Roux-en-Y gastric bypass and sleeve vertical gastrectomy: an integrative review. Arq Bras Cir Dig 2018;31(4):e1400.

[41]. Könner AC, Brüning JC. Toll-like receptors: linking inflammation to metabolism. Trends Endocrinol Metab 2011;22(1):16–23. [PubMed: 20888253]

[42]. Sala P, Torrinhas RSMM, Fonseca DC, et al. Intestinal expression of toll-like receptor gene changes early after gastric bypass surgery and association with type 2 diabetes remission. Nutrition 2020:79–80.

[43]. Petersen C, Bell R, Klag KA, et al. T cell-mediated regulation of the microbiota protects against obesity. Science 2019;365(6451). 10.1126/science.aat9351.

[44]. Caesar R, Tremaroli V, Kovatcheva-Datchary P, et al. Crosstalk between gut microbiota and dietary lipids aggravates WAT inflammation through TLR signaling. Cell Metab 2015;22(4):658–68. [PubMed: 26321659]

Editorial comment

Comment on: Toll-like receptor 4 and MyD88 are required for gastric bypass-induced metabolic effects

Bariatric and metabolic surgery is the most effective treatment for severe obesity, type 2 diabetes, and co-morbidities. Roux-en-Y gastric bypass (RYGB) is one of the most performed procedures, which has sustained effects on weight loss. The mechanisms underlying the benefits of RYGB are unclear.

Obesity is characterized by metabolic endotoxemia, a condition defined as a low-grade elevation of plasma lipopolysaccharide (LPS) concentration. A high-fat diet enriched in saturated lipids induces metabolic endotoxemia and plays a causal role in the development of obesity and metabolic syndrome, which is attenuated by toll-like
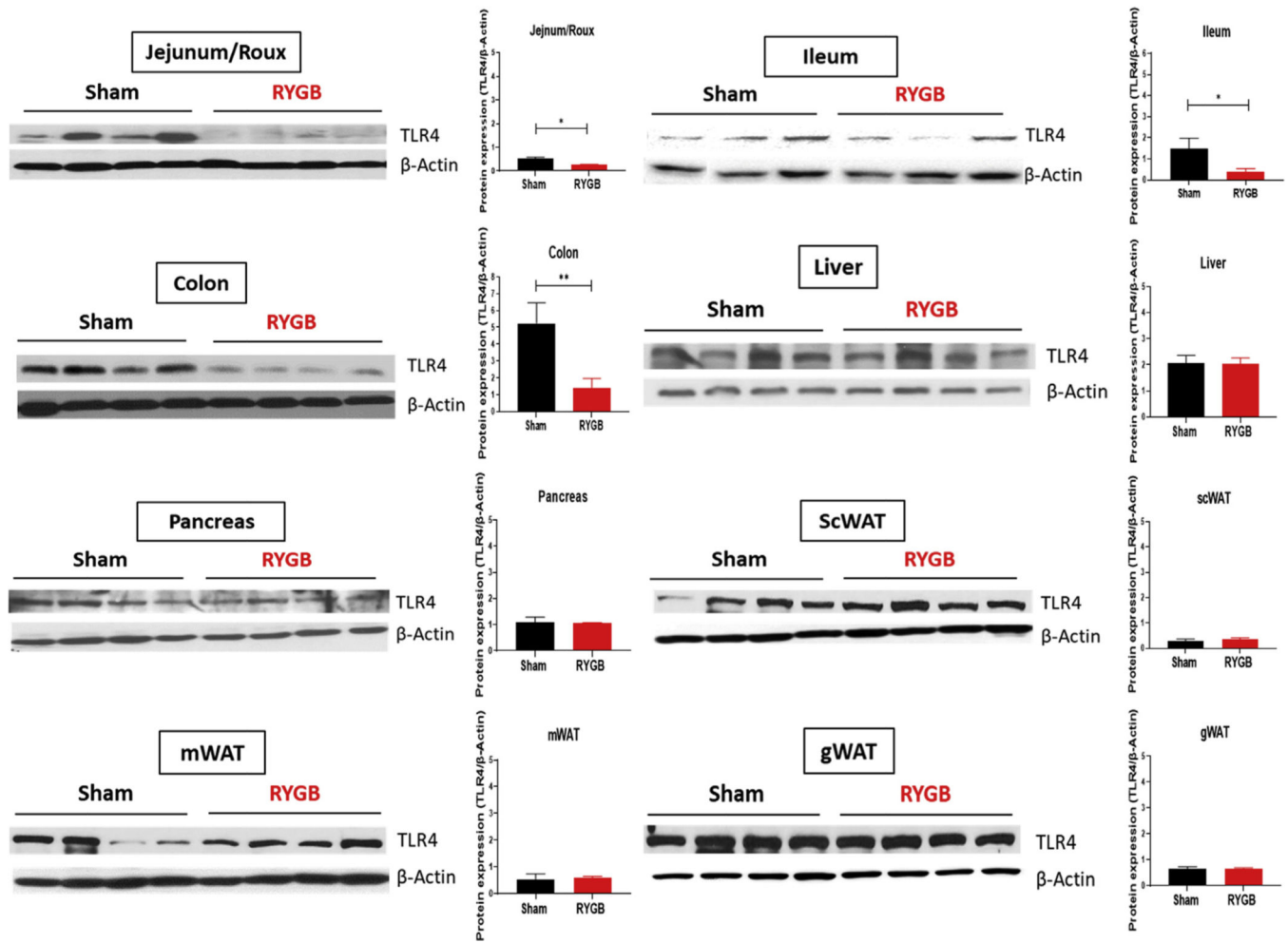
Fig. 1.
TLR4 expression is decreased in the intestines of RYGB-operated obese mice. TLR4 expression by Western blot in jejunum (or Roux limb), ileum, colon, liver, pancreas, subcutaneous (sc), WAT, mesenteric (m) WAT, and gonadal (g) WAT of sham- and RYGB-operated HFD-induced obese male C57 Blc/6J mice. β-actin is serving as a loading control. n = 3–4.
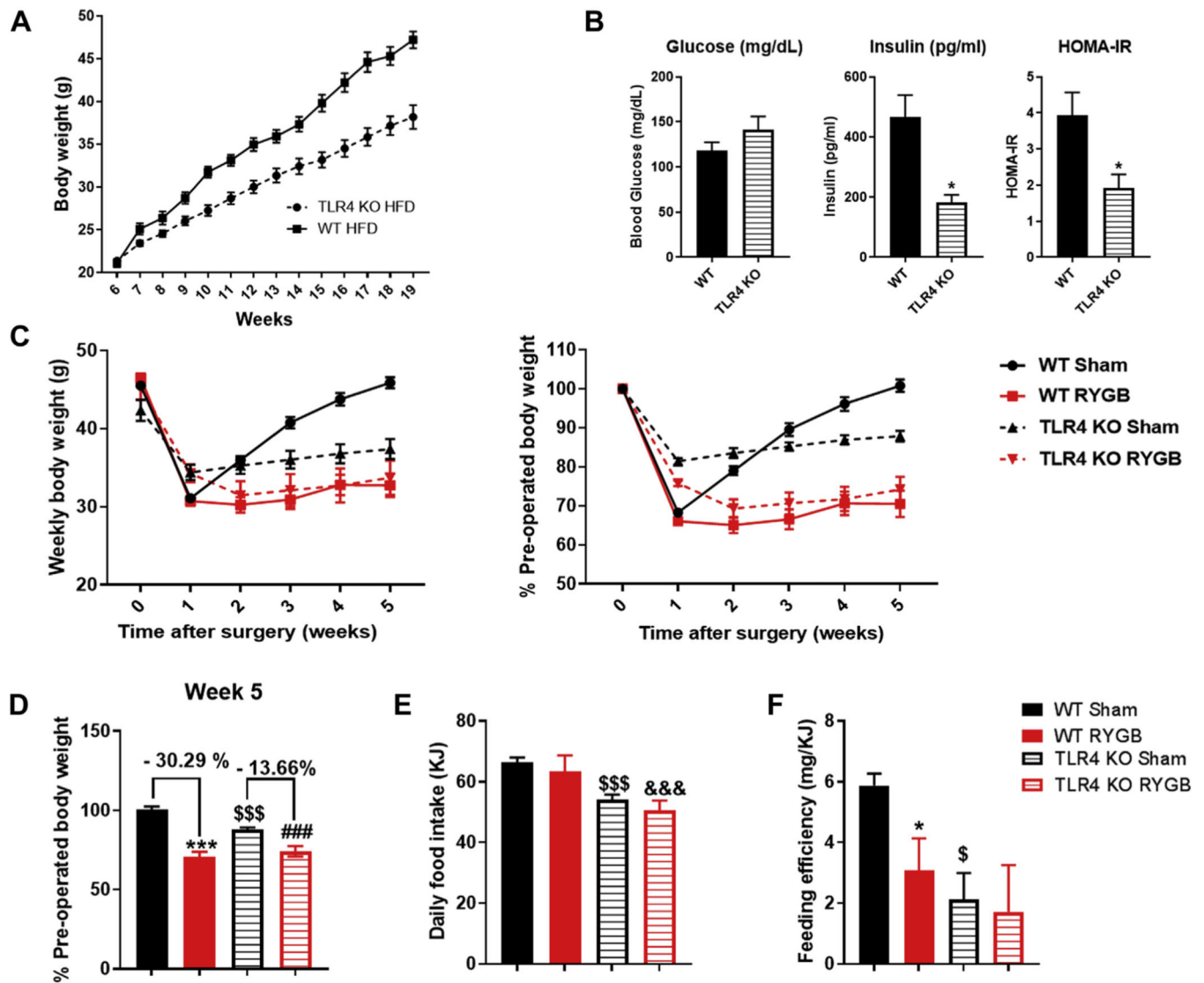
Fig. 2.
TLR4 KO mice have an attenuated weight loss response to gastric bypass. (A) Weight change in grams in TLR4 KO mice compared to WT mice on HFD over 13 weeks after weaning. (B) Measurement of fasting blood glucose, fasting insulin, and homeostatic model assessment for insulin resistance in WT mice and TLR4 KO mice at weeks 18 and 19 postweaning. n = 22–26. *P< .05. (C) Average weight change in percentage (left) or weight in grams (right) over 5 weeks in WT sham, WT RYGB, TLR4 KO sham, and TLR4 KO RYGB mice. (D) Weight change at week 5 after surgery in WT and TLR4 KO mice (expressed as percentage preoperative weight). (E) Average daily food intake for all groups. (F) Feeding efficiency in (mg/KJ) for all mice groups. Two-way ANOVA was used to compare mean across all 4 groups. WT sham/RYGB n = 7–8, TLR4 sham n = 16, RYGB n = 8. *,$ P<.05, ***, ###, &&&, $ $ P<.001. *WT sham versus WT RYGB, #TLR4 KO sham versus TLR4 KO RYGB, $WT sham versus TLR4 *KO* sham, &WT RYGB versus TLR4 KO RYGB.
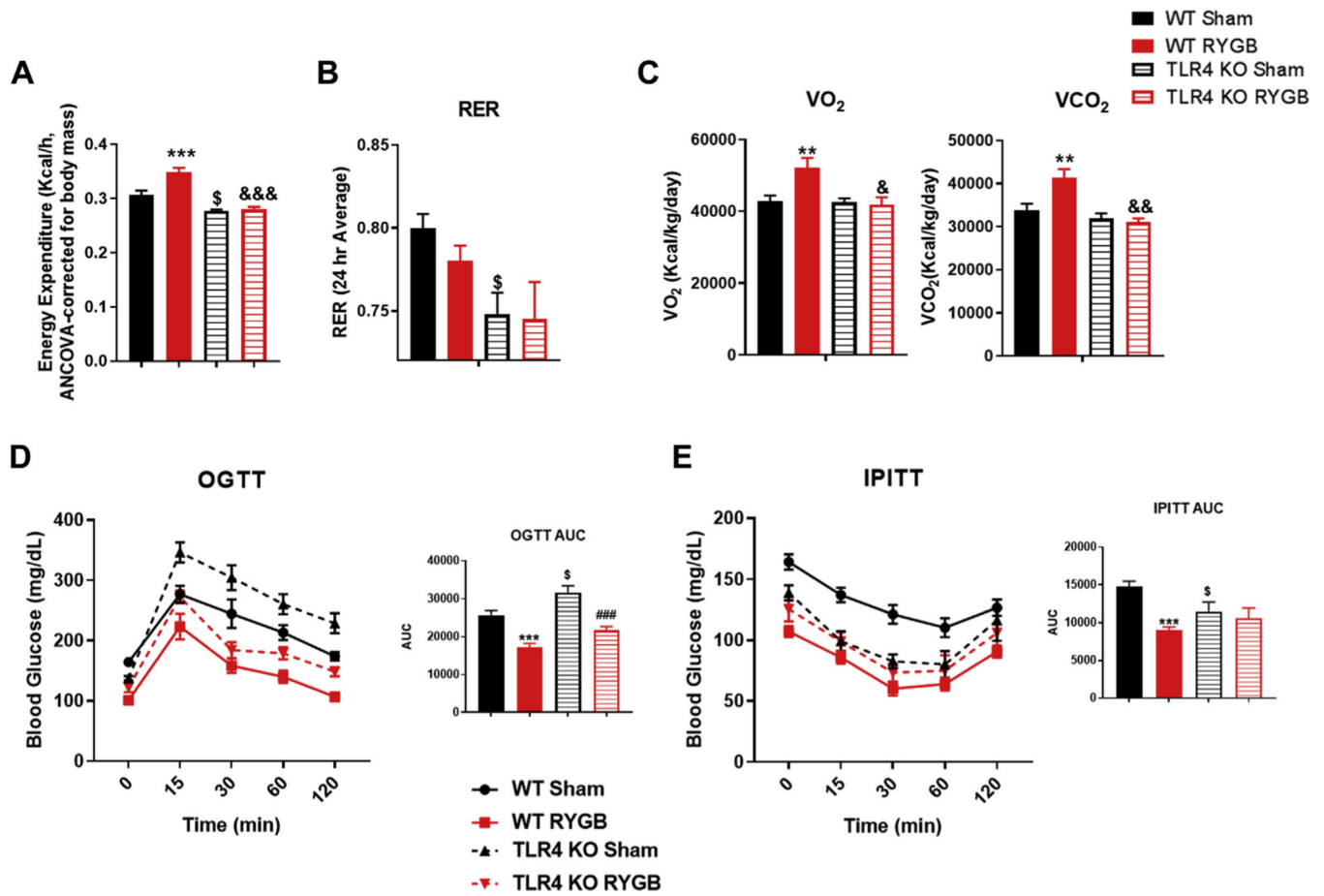
Fig. 3.
TLR4 is required for RYGB-mediated increase in energy expenditure and improvement in glucose homeostasis. (A) Energy expenditure in WT and TLR4 KO mice after surgery. (B) Respiratory exchange ratio for all groups. (C) VO_2 and VCO_2 for all groups. (D) Oral GTT and (E) intraperitoneal ITT in WT sham, WT RYGB, TLR4 KO sham, and TLR KO RYGB mice. WT sham/RYGB n = 7–8, TLR4 KO sham n = 16, TLR4 KO RYGB n = 8. Two-way ANOVA was used to compare means between the 2 genotypes based on the surgery intervention variable. $^{\$}P < .05$, **, $^{\&\&}P < .01$, ***, $^{\#\#\#}P < .001$. *WT sham versus WT RYGB, $^{\#}$TLR4 KO sham versus TLR4 KO RYGB, $^{\$}$WT sham versus TLR4 KO sham, $^{\&}$WT RYGB versus TLR4 KO RYGB.
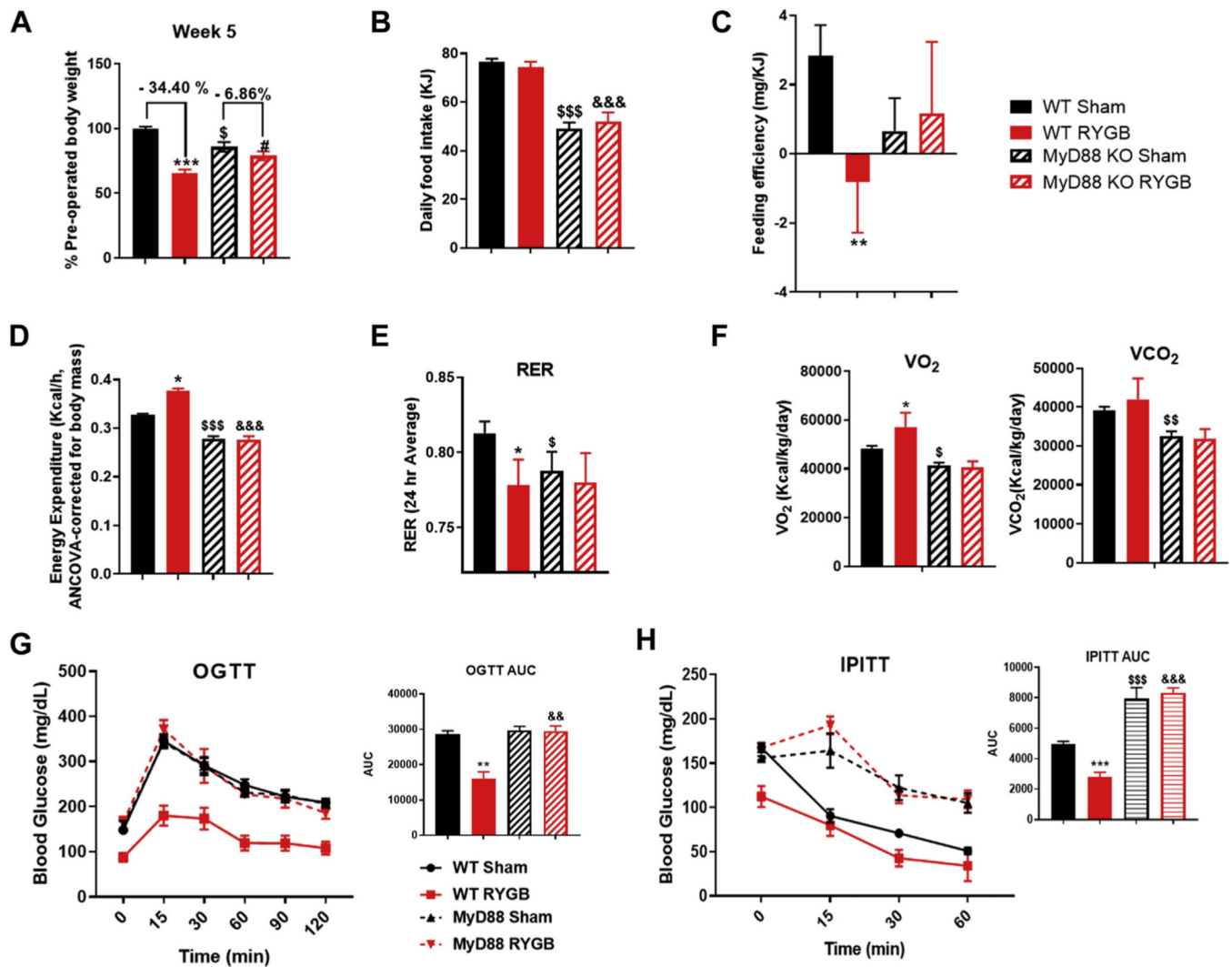
Fig. 4.

MYD88 is required for all RYGB-induced metabolic effects. (A) Average weight change in percentage over 5 weeks in WT sham, WT RYGB, MyD88 KO sham, and MyD88 KO RYGB mice. (B) Average daily food intake for all groups. (C) Feeding efficiency in (mg/KJ) for all mice groups. (D) Energy expenditure in WT and MYD88 KO mice after surgery. (E) Respiratory exchange ratio for all groups. (F) VO_2 and VCO_2 for all groups. (G) comparing oral OGTT in WT mice sham and RYGB and MyD88 KO sham and RYGB. (H) Intraperitoneal ITT in all groups. Two-way ANOVAwas used to compare means between the 2 genotypes based on the surgery intervention variable. WT sham n = 11, RYGB n = 11, MyD88 KO sham n = 5, RYGB n = 5. *, [#], [$]$P$<.05, **, [$$], [&&]P<.01, ***, [$$$], [&&&]P <.001. *WT sham versus WT RYGB, [#]MYD88 KO sham versus MYD88 KO RYGB, [$]WT sham versus MYD88 KO sham, [&]WT RYGB versus MYD88 KO RYGB.
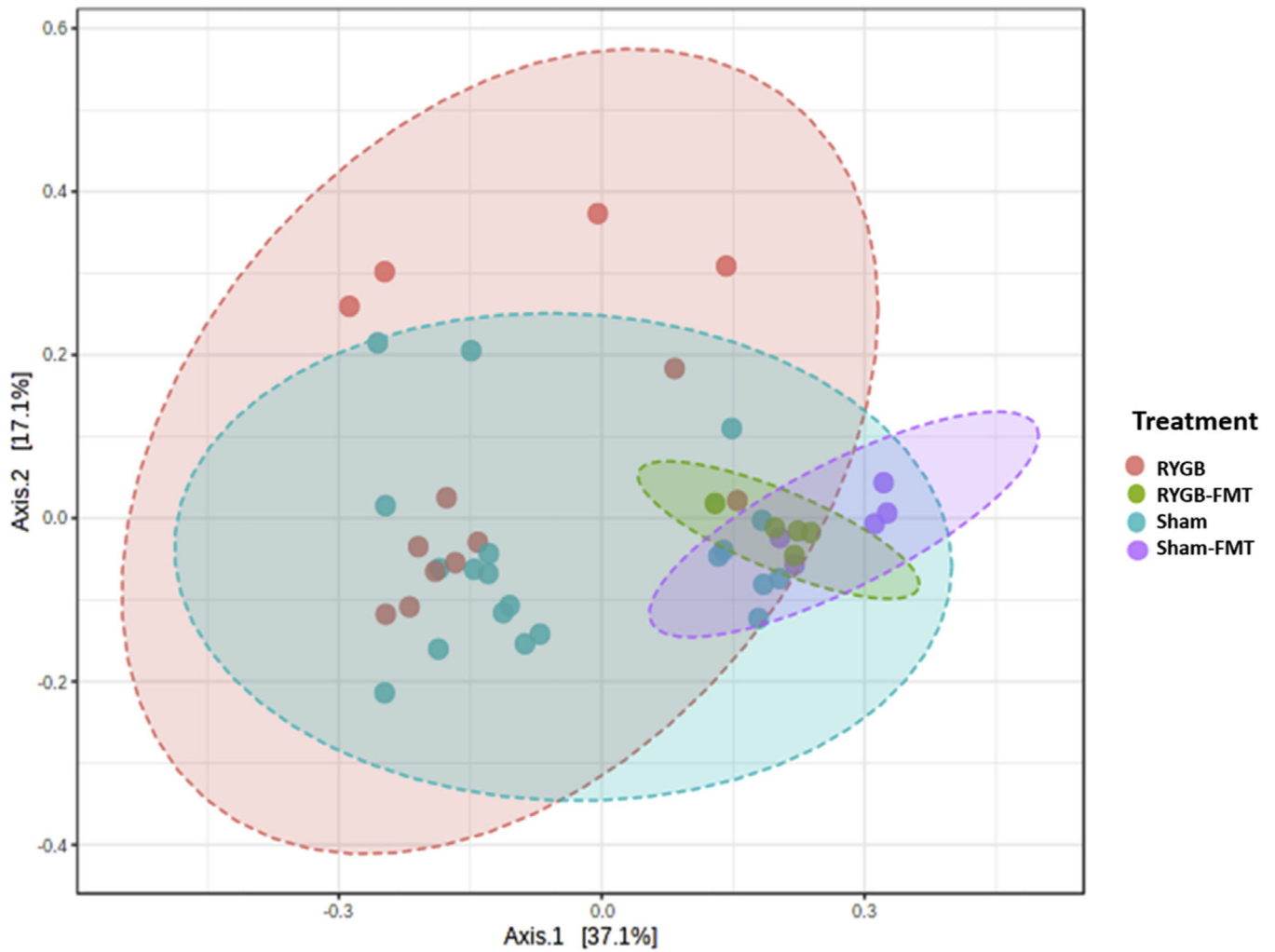
Fig 5.
Principal coordinate analysis of beta-diversity using Euclidian distance from RYGB mice, WT mice receiving FMT from RYGB mice (i.e., RYGB-FMT), sham mice, and WT mice receiving FMT from sham mice (i.e., sham-FMT). Each dot represents bacterial composition within a single mouse while color represent different groups. The figure was generated using MicrobiomeAnalyst.
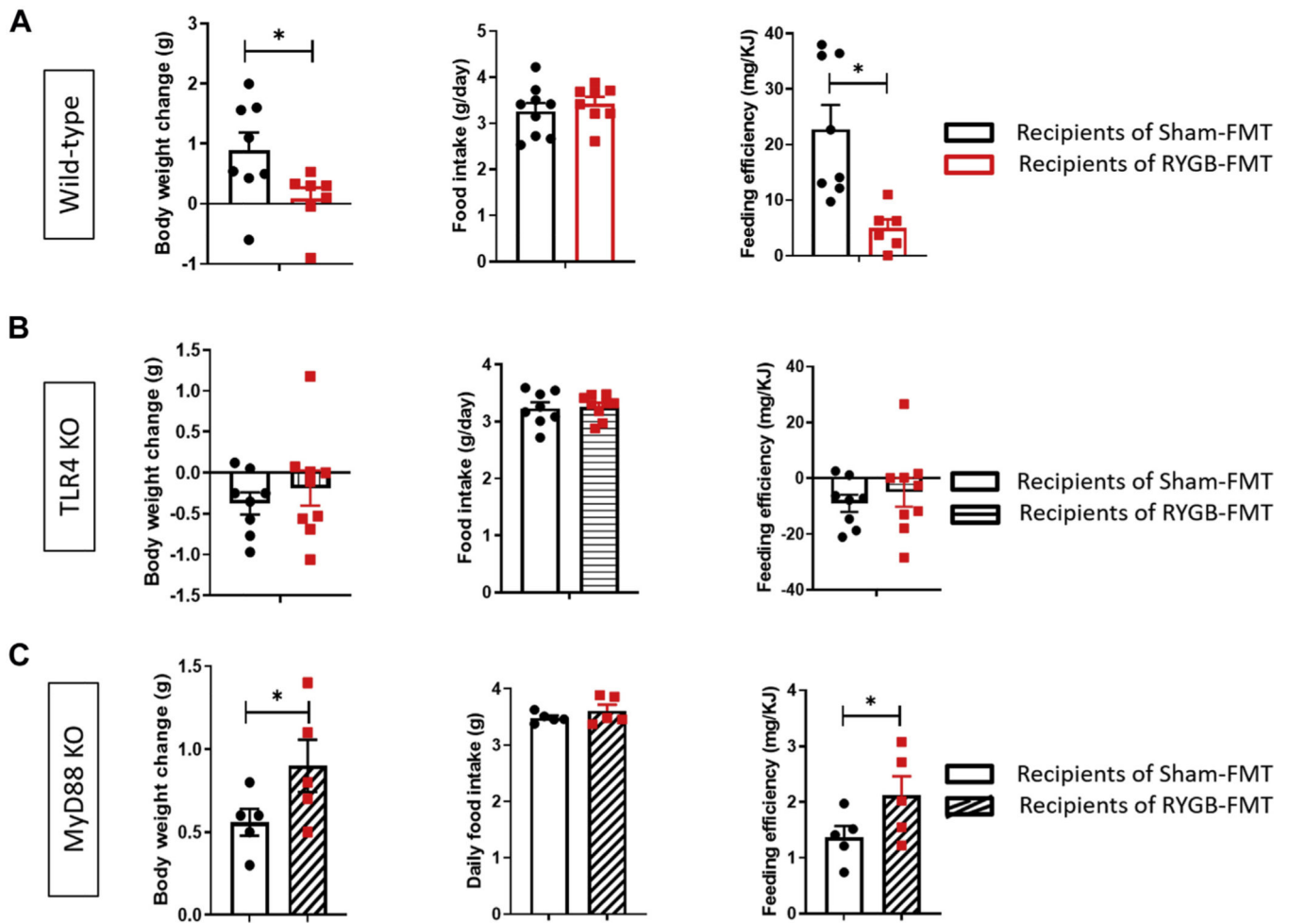
Fig. 6.

TLR4 and MyD88 are required for weight loss induced by RYGB-derived FMT. Weight change (g), food intake measurement (g/chow/day, and feeding efficiency (mg/KJ) in (A) wild-type (WT), (B) TLR4 KO, and (C) MyD88 KO mice receiving FMT from sham-versus RYGB-operated animals. Student's *t* test. n = 5–8. *$P < .05$.